

# 3D INSPECTION SYSTEM IN CERAMIC TILES SURFACES WITH RANGE IMAGES

G. Pabón-Rodríguez, G. Andreu-García, A. Rodas-Jordá  
J. Valiente-González and F. Acebrón-Linuesa  
*Computer Vision Group, Universidad Politécnica de Valencia, Spain*

**Keywords:** Surface inspection, Computer vision system, 3D defect detection, Quality control, Range images.

**Abstract:** In this paper we propose a system to characterize 3D defects of range images, which can be combined with traditional surface inspection methods in an industrial environment for ceramic tiles inspection. Our application has the advantage of learning the geometric features of the ceramic pieces, creating a unique 3D model against which we compare the test pieces. In addition to this, the system includes a robust learning phase, which discards tiles with defects impossible to see from a human expert and a more stringent inspection in areas with low uncertainty. Experiments with real data were performed. Our data consist of tiles of different types, shapes and silk-screen of ceramic tiles. Results are promising for tiles with a straight orientation, over 99 % of defects are correctly classified.

## 1 INTRODUCTION

This paper is concerned with the problem of automatic inspection of ceramic tiles using computer vision. Our objective is to propose a suitable vision system to detect and quantifier topographic surface defects in tiles with nonplanar surfaces, irregular shapes and glazed surfaces.

Decorative ceramic tile are manufactured in vast quantities. According to (Smith, 2000) a large range of tile designs are currently produced. These tiles can have different shapes varying from conventional simple planar designs to highly complex three-dimensional forms and, in finish, from uniform color to irregular pseudo-random designs or natural random patterns typical of polished stone.

Most of ceramic tile automated inspection system have predominantly been aimed at the inspection of planar tile surfaces of uniform colouring. The detection of defects in the case of nonplanar tiles or tiles with pseudo-random patterns is more complex. In (Boukouvalas et al., 1995) a successful application of various image analysis techniques for the inspection of uniform planar tiles is described. In the case of more complex patterned planar tile designs, an off-line training stage has been proposed in order to detect in both regular and random patterns. However, such an approach is not able to explicitly distinguish three-dimensional topographic, from two-

dimensional chromatic defects.

An automatic system to inspect and classify ceramic tiles according to the integrity defects at the tile corners is described in (Valiente et al., 1998). The system detects the lack of material in the corner of the tile basing on the differences of color among the zone damaged and the remainder of tile, but if the zone where there is a lack of material has been colored the system does not work correctly.

Almost all the methods revised, like (Boukouvalas et al., 1999), (Boukouvalas and Petrou, 2000), (López et al., 2001) and (López et al., 2005) detect chromatic defects but not topographical ones. In (Smith, 2000) a technique that is able to isolated mixed topographic and chromatic surface features has been developed. They proposed a photometric stereo technique for the acquisition of quality data in the inspection of ceramic tiles, possessing both topographic and albedo features. The method is able to separate a surface topographic description from a coincident albedo pattern. In the paper does not expose any method to quantify the defects.

Our goal is to propose a suitable computer vision system to detect and obtain measures of magnitude of topographic surface defects. The system has to inspect all the surface and to work with nonplanar surfaces, irregular shapes and glazed surfaces. The system has to offer solutions that can be used in real world, this is in ceramic industry. A supervised ap-

proach to classifier requires a great number of defective samples, which can be difficult to obtain. So we need to implement an inspection method based only in good samples for training purpose. Contrary to supervised classification novelty detection only need normal samples. With novelty detection method the system will have the advantage of being able to detect new types of defects that were unknown at the time of training.

In our proposed, a pattern 3D is obtained to each tile model with uncertainly criterion that permit taking account the real inaccuracy in tile manufacturing. Edge detection, matching and image registration techniques to align tiles are used. Finally generates a 3D pattern of a defect-free ceramic tile and via novelty detection the defects are identified. Experiments with commercial tiles show the good system performance.

## 2 ACQUISITION ENVIRONMENT

The surface inspection requires acquiring images that are more suitable than the human visual perception. Range images are a special class of digital images. A range image reproduces the 3D structure of a scene. Currently exists a variety of range measuring technologies to acquire 3D information about our world. Laser range scanners can provide extremely accurate and dense 3D measurement over a large working volume.

Our acquisition system is located in an opaque box to not be affected by external light and put together a commercial acquisition system based in ranger C55 camera, linear laser of 635nm and a conveyor belt. The ranger C55 can be classified as MultiScan camera where high speed 3D and gray-scale data are output according to the line scan method. The object is illuminated from a position angle 45 degrees with a laser line projector and viewed with the camera from a position on vertical to conveyor belt, see Figure 1. The

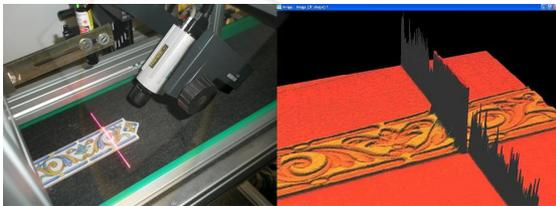


Figure 1: Left image represents the acquisition environment camera, conveyor belt and lineal laser light. In the right image can see the 3D line projection on tile.

lineal profiles acquired to obtain 3D shapes are based on the method called laser triangulation. Ranger C55

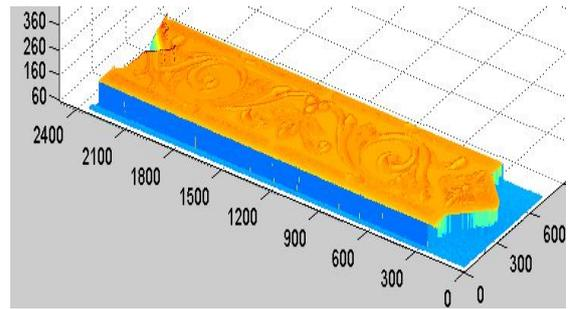


Figure 2: Example of 3D image tile obtained with our environment acquisition.

resolution is 1536\*512 pixels and can acquired until 35000 profiles per second.

An example of the 3D image tile used in this work can see in Figure 2. The images used in this work are acquired while the conveyor belt was working and with a final resolution of 0.06 mm in the Z direction (direction vertical to conveyor belt).

## 3 VISUAL INSPECTION VIA NOVELTY DETECTION

Supervised classification has been demonstrated as a powerful approach when both training data and testing data are well-conditioned. However, supervised approach often involves a lengthy training stage and, more importantly, it requires a substantial number of defective samples, which for some applications can be difficult to obtain.

In a novelty detection task, the classifiers task is to identify whether an input pattern is part of the data or it is in fact unknown. As for defect detection, it involves assigning a normal or abnormal label to a pattern (e.g. a surface or a pixel). Contrary to supervised classification, novelty detection only needs the normal samples for training purposes and usually uses a distance measure and a threshold for decision making. Recently, (Markou and Singh, 2003) gave a detailed review of novelty detection approaches, using statistical and approaches.

Statistical parametric approaches are commonly used in visual inspection (Xie, 2008). The fundamental assumption is that the data distribution is Gaussian in nature. Each pattern is usually represented as a point in a d-dimensional feature space, where d is the length of the feature vector. The objective is then to establish decision boundaries in the feature space and reject patterns that fall in regions of low density. The decision boundaries are determined by the probability distribution of the patterns at training stage.

The available performance measure for novelty detection methods is the probability of false positives (FP) that is rejection of good samples. Increasing the acceptance decision boundary will then obviously decrease the risk. However, it is also clear that the probability of false negatives depends on the acceptance region. In some applications, the decision boundary is simply set as the maximum range of normal samples in the training stage.

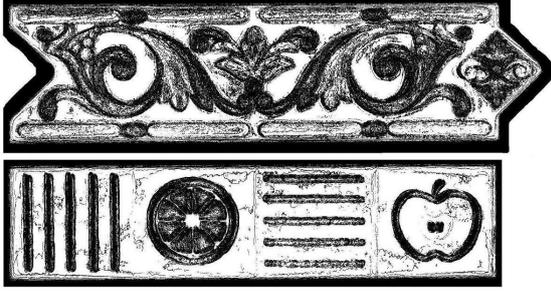


Figure 3: Uncertainty image  $U$  obtained for arrow and apple models. The darker areas indicate greater uncertainty and the white area shows the areas marked as smoothing areas by our system.

### 3.1 The 3D Tile Pattern

The aim is to obtain a 3D tile pattern with ability to discriminate defective tiles and accept at the tiles considered non-defective. All tiles with free surface defects and those tiles with subtle changes on original design must be considered as non-defective tiles.

The tiles are manufactured automatically and the ornamental designs are stamped on them with a relative accurate. Due to this fact there is no a precise correspondence between points with the same coordinates of two tiles, but most likely if there is correspondence with points in your neighborhood. This disagreement between regular samples is referred by us as inter-discrepancy between samples, but it is not considered as defects.

Another direct consequence of the manufacturing process is that the material is not distributed with precisely on the surface. Small differences in the amount of varnish not affect the quality of tile but if it computes the absolute differences between two tiles then it could be detected as defects. This fact is referred by us as intra-discrepancy.

These aspects force us to implemented a pattern that has account the uncertainly. Only true regular tiles samples (free-defect) can be used to obtained a 3D pattern. The use of the window concept and Neighborhood criteria allow us to successfully addressing the inter-discrepancy and make an analysis of how smooth or rough are the decorative designs,

this aspect is necessary to obtain measurements of the intra-discrepancy. These two aspects are not considered real defects but inequalities of the production process.

Let a  $T^i$  range image that represents a tile, it denotes by  $t_{lk}^i/t_{lk}^i \in T^i$  the profile obtained to pixel with coordinates  $(l, k)$  in the plane  $(x, y)$  of the image. Setting a  $3 \times 3$  window pixels, it denotes by  $N_{lk}^i$  the 8-nearest neighbor to pixel with coordinate  $(l, k)$  included itself. For each  $T^i$  one image of intra average  $A^i$  is computed using a  $3 \times 3$  window, then each element  $a_{lk}^i \in A^i$  can be computed as:

$$A^i = \left\{ a_{lk}^i \mid a_{lk}^i = \frac{1}{9} \sum_{(p,q) \in N_{lk}^i} t_{lk}^i \right\} \quad (1)$$

In a similar way, for each  $T^i$  one image of intra maximum  $X^i$  and one image of intra minimum  $M^i$ , using the  $3 \times 3$  window, are obtained as follow:

$$X^i = \left\{ x_{lk}^i \mid x_{lk}^i = \max(t_{pq}^i \mid \forall t_{pq}^i \in N_{lk}^i) \right\} \quad (2)$$

$$M^i = \left\{ m_{lk}^i \mid m_{lk}^i = \min(t_{pq}^i \mid \forall t_{pq}^i \in N_{lk}^i) \right\} \quad (3)$$

The criterion to detect defect cannot be equal to all tile surface. In tile regions with smooth decorative elements a severe criterion can be used. But in rough regions, regions with wave or regions with many edges the criterion has to be smoothing to avoid false detection. In order to identify the smoothing of the regions a binary image  $S^i$  will be used to implement the pattern, the elements  $s_{lk}^i \in S^i$  are computed as:

$$s_{lk}^i = \begin{cases} 1, & \text{if } \sum_{(p,q) \in N_{lk}^i} (t_{lk}^i - t_{pq}^i) = 0 \\ 0, & \text{if } \sum_{(p,q) \in N_{lk}^i} (t_{lk}^i - t_{pq}^i) \neq 0 \end{cases} \quad (4)$$

The criterion of above expression is: if the 8-nearest neighbors have the same value then the region is considered as an homogeneous region. This can see a very restrictive criterion but is important to be sure about the variability that is appropriate to tolerate in each zone tile

Two aspects are taken into account to design the uncertainly image  $U$ ; the intra-discrepancy through the  $A^i$  and  $A^j$  images and la inter-discrepancy through the  $S^i$  and  $S^j$  images. The images  $U$  can be defined as,

$$U = \left\{ u_{lk} \mid u_{lk} = \frac{1}{n} u_{lk}^{ij} \right\} \quad (5)$$

being  $n$  the number of true samples selected to compute the uncertainly image and the  $u_{lk}^{ij}$  values obtained as,

$$u_{lk}^{ij} = \max_{1 \leq j \leq n} \left[ \sum_{j+1 \leq i \leq n} C(a_{lk}^j - a_{lk}^i) (s_{lk}^j \wedge s_{lk}^i) \right] \quad (6)$$

where,

$$C(x) = \begin{cases} 1, & \text{if } x = 0 \\ 0, & \text{if } x \neq 0 \end{cases} \quad (7)$$

The values of the  $u_{lk}^{ij}$  pixels represent the amount of regular tiles that have voted this area as homogeneous. The uncertainly image  $U$  is a measurement about how many training tiles (without defect) consider that a tile region is homogeneous. Examples of uncertainty image can see in figure 3, where white area are homogeneous region.

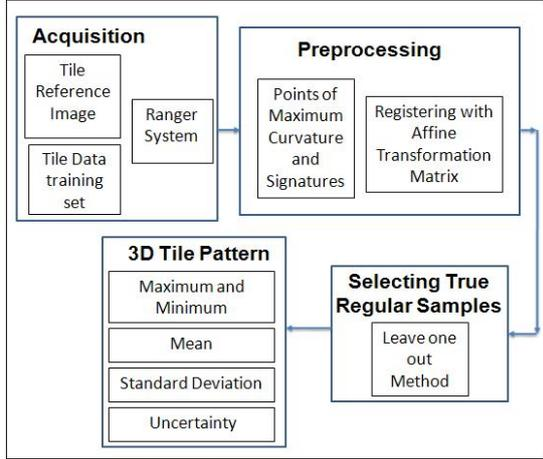


Figure 4: Sequence of steps to obtain 3D pattern  $\Omega$ .

Let a training set data of tiles and their ranger image set  $T = \{T^i\}_{i=1}^n = \{T^1, \dots, T^n\}$ , and evaluated the corresponding  $A^i, X^i, M^i$  and  $S^i$ , the images  $A, D, X$  and  $M$  can be deduced as follow,

$$A = \left\{ a_{lk} \mid a_{lk} = \frac{1}{n} \sum_{i=1}^n a_{lk}^i \right\} \quad (8)$$

$$D = \left\{ d_{lk} \mid d_{lk} = \frac{1}{n} \sqrt{\sum_{i=1}^n (a_{lk} - a_{lk}^i)^2} \right\} \quad (9)$$

$$X = \left\{ x_{lk} \mid x_{lk} = \max_{1 \leq i \leq n} (x_{lk}^i) \right\} \quad (10)$$

$$M = \left\{ m_{lk} \mid m_{lk} = \min_{1 \leq i \leq n} (m_{lk}^i) \right\} \quad (11)$$

The  $\Omega$  pattern can be set as a set of five images  $\Omega = \{A, D, X, M, U\}$  that representing the images of the average, the deviation standard, the maximum, the minimum and the uncertainty. The figure 4 shows a diagram with the steps necessary to obtain the pattern. An aspect very important is how can be selected the set tile  $T$  appropriated to obtained the  $\Omega$  pattern.

### 3.2 Selecting True Regular Samples

A selecting true regular samples process previous to obtain the pattern is take out. The objective of this

process is to select between the classified tiles as regular tiles (free-defect) by the human operator that, one time are evaluated by the vision system, also will be considered as regular tiles. The tiles that satisfy the above criterion are referred by us as true regular samples. Obviously those tiles that are in the final selection are tiles with a minimal inter-discrepancy between them. The figure 4 shows all the process.

Considering a set  $T = \{T^1, \dots, T^m\}$  of regular samples candidates to be selected as regular true samples, a subset of  $m - 1$  pseudo-pattern  $\Psi = \{\Psi^1, \dots, \Psi^{m-1}\}$  are obtained where  $\Psi^i$  is computing using all the samples of the  $T$  set except the sample  $i$  in a process of leaving-one-out.

Each  $\Psi^i$  is defined as  $\Psi^i = \{A^{\Psi^i}, D^{\Psi^i}\}$  where  $A^{\Psi^i}$  and  $D^{\Psi^i}$  are obtained using the expressions (8) and (9) respectively and with  $m - 1$  samples.

For each sample  $T^i$  a discrepancy map  $R^i$  is obtained using the pseudo-pattern  $\Psi^i$ . The discrepancy map to  $R^i$  can be deduced as follow:

$$r_{lk}^i = \begin{cases} 0, & \text{if } (a_{lk}^{\Psi^i} - d_{lk}^{\Psi^i}) \leq t_{lk}^i \leq (a_{lk}^{\Psi^i} + d_{lk}^{\Psi^i}) \\ 1, & \text{in other case} \end{cases} \quad (12)$$

The pixels with  $r_{lk}^i = 0$  are considered no-disagree. If all the pixels of tile  $T^i$  have been considered as no disagree then  $T^i$  is a true regular samples and  $T^i$  will selected to figure up the pattern  $\Omega$ . In other case when  $\exists r_{lk}^i \in R^i \mid r_{lk}^i \neq 0$  the  $T^i$  is rejected to compute the pattern  $\Omega$ .

Rectangle Test N° 8 Image Size: 3500 x 1416 4.956.000 pixels				Tile Size : 1.053.894 pixels Defects: 9.063 pixels Rate Defects: 0.86 %		
Color	Volume	area	perimeter	dispersion	Uncertainty	defect weighting
Yellow	39109	5314	336	21	66%	25811,94
Magenta	27130	3752	307	25	76%	20618,8

Figure 5: A numerical example of different values to estimate the defects.

### 3.3 Defect Maps

For each test tile a defect maps  $\Theta^i$  is obtained using the pattern  $\Omega = \{A, D, X, M, U\}$  defined in previous sections.

Given  $T^i$  a data test and  $\Omega$  the 3D tile pattern, the step in order to obtain the defect maps  $\Theta^i$  is as follow:

Step1. Compute  $A^i, X^i$ , and  $M^i$ , applying (8), (10) and (11).

Step 2. Estimate  $R^i$  from  $A^i$  and  $D^i$ , applying (12).

Step 3. Calculate  $\theta_{lk}^i \in \Theta^i$  as follow:

$$\theta_{lk}^i = \begin{cases} 0, & \text{if } m_{lk}^i \leq t_{lk}^i \leq x_{lk}^i \\ r_{lk}^i (x_{lk}^i - t_{lk}^i), & \text{if } t_{lk}^i > x_{lk}^i \\ r_{lk}^i (m_{lk}^i - t_{lk}^i), & \text{if } t_{lk}^i < m_{lk}^i \end{cases} \quad (13)$$

Then  $\Theta^i$  is an image than contain pixels to zero and pixels greater than zero. The pixels  $\theta_{lk}^i \in \Theta^i$  are pixels defects free if  $\theta_{lk}^i = 0$ , in other case, the pixels with  $\theta_{lk}^i > 0$  are pixel with defects and the positive value is the first approximation to quantify the defect.

Obtained  $\Theta^i$  the image  $U$  is used to weigh the defects. The aim is that small values in  $\Theta^i$  are very significant if its on smoothing area and on rough area only big values are considered as defect. In this sense the image  $U$  is considered with an image of weights.

To remove noise in  $\Theta^i$  a morphological operator was applied, with a disk shape of radius 5 pixels as structuring element. Finally the defect pixels are clustered with criterion of 8-connected pixels and a measurement about the defect area is obtained. An example of this region is shown in figure 5. Considering this area, and the profiles of pixels inside of area, a measurement of volume of defects is estimated. Using the measurement of volume and area and the image  $U$  different criteria to quantify and to classify the defects can be thought out.

## 4 EXPERIMENTS AND RESULTS

For the experiments was necessary to set up an image database based on real samples from the tile industry. We have used in our experiment a data set of 210 tiles extracted directly from the factory, the production line, so we work with real data and real defects. The database is comprised by two model named for us "arrow" and "apple", see figure 6. We considered these two models appropriate to test our proposal, because its have different forms and contain on its surface as smooth as rough areas.

Table 1: Composition and distribution of tiles in the database used in the experiments.

Tile Model	Pattern tiles	Test free defect	Test with defect	Total tile
Arrow	13	35	63	111
Apple	8	31	60	99

For each tile model, arrow and apple, a process of selecting true regular samples was carried out, as is described in section 3.2. Table 1 shows the tile distribution for each model in database, in this table can see a total of 111 arrow tiles and 99 apple tiles was used. At the beginner of the selecting process 15 free defect

Table 2: Summary result.

Tile	degree	TP %	TN %	FP %	FN %
Arrow	0°	100	98.4	0	1.6
	10°	97.9	95.2	2.1	4.8
	-10°	100	95.2	0	4.8
Apple	0°	100	100	0	0
	10°	89.7	96.7	10.3	3.3
	-10°	94.8	93.3	5.2	6.7

tiles was candidate to obtain the the 3D pattern but after of the selecting process only 13 arrow tiles and 8 apple tiles were used to compute the pattern  $\Omega$  the other free defect tiles was used to test the system. The defect of test samples was lumps, depressions, orange peel, material lack and too varnish.

Three different orientations were taken into account to do the experiments: i) 0 degree, this is the best position to acquire images during the test and implies that the tiles will be placed on the conveyor belt completely parallel to the bands. ii) 10 degree, this implies that the tiles it is placed an angle  $\alpha$  to the central of belt such that  $0 < \alpha \leq 10$ . iii) -10 degree, this implies that the tiles it is placed an angle  $\alpha$  to the central of belt such that  $0 > \alpha \geq -10$ .

In all stage of the process three orientation was taken into account for thus, pattern  $\Omega$  will be projected to three orientations so three different patterns were obtained for each model  $\Omega^{10^\circ}$ ,  $\Omega^{0^\circ}$  and  $\Omega^{-10^\circ}$  and all the test on the tiles were repeat for each orientation. During the test process the system select automatically the pattern with the more appropriate orientation have account the orientation of test data.

The increment of FP and FN in the rotated tiles are due to greater deformation that is produced at the laser line in capture stage.

All test pieces were successfully tested by the system; the results were summarized in table 2. In test stage, for each tile it image is acquired and the processing steps represented in figure 4 are made as follow:

i) The tile contour (signature) is computed in order to find differences between the angles of the test images and pattern tiles. The maximum curvature points are control points to generate a transformation matrix and determine the correspondence between the test tile points and the three pattern of model.

ii) Knowing the coordinates of a set points in the test tile image, an affine transformation (Gottesfeld, 1992) is determined to re sample the geometry of the test tile image.

A detailed performance is showed in Table 2 where the detection rate for each model is presented as: true positives (TP), false positives (FP), true neg-

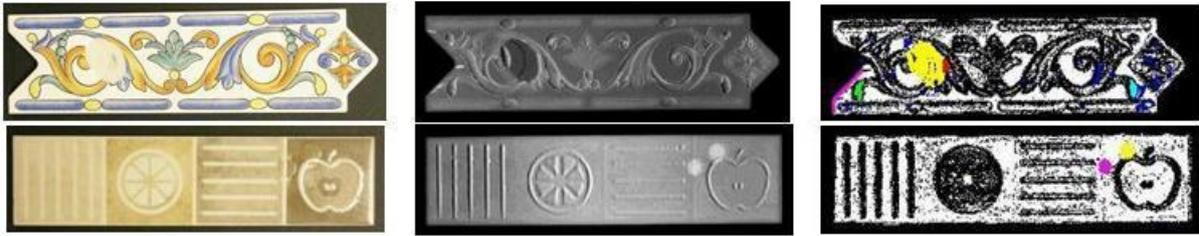


Figure 6: From left to right: Original tiles, Range images and Defect marked on uncertainty image.

atives (TN) and false negatives (FN). This approach keeps the success rate on expected levels, but decreases to 94% when test tiles is rotated. The weight factor of a defect increases when its position is between areas of high and low uncertainty, see figure 5.

Our proposed approach add the quantification of detected defects in contrast to other systems e.g. (Smith, 2000). We achieved our goal inspecting the entire surface of tiles and to work with no planar surfaces, irregular shapes and glossy or glazed surfaces.

The proposed system has a final resolution of 0.06 mm in the Z direction. This extracts a set of features: quantity of defective pixels tile, centroid, bounding box, area, volume, perimeter, confidence measure, and dispersion each tile defect. Also, it can detect silk-screened defects because the color affects some depth measurement. Experiments with commercial pieces show reconstruction errors caused by the combination of color and varnish.

## 5 CONCLUSIONS

A system for industrial inspection of ceramic tiles is presented, showing a sophisticated inspection strategy, with promising results. The proposed algorithm use range images, to improve small defects detection so difficult to see for human eyes.

Our algorithm is aimed to characterize 3D defects of range images with novelty detection tasks, which that only needs the normal samples for training purposes and usually uses a distance measure and a threshold for decision making. We tested successfully the algorithm in some orientations with test tiles from different shapes and textures. With novelty detection method the system will have the advantage of being able to detect new defects that were unknown at the time of training.

Our future efforts: improve the response of the algorithm about color, shadows, brightness effects and time response time. This will include a stage that automatically corrects the false measurements deep in the 3D reconstruction.

## ACKNOWLEDGEMENTS

This work has been supported partially by research project DPI2007-51166596-C02-01 (VISTAC).

## REFERENCES

- Boukouvalas, C., Kittler, J., Marik, R., Mirmehdi, M., and Petrou, M. (1995). Ceramic tile inspection for color and structural defects. In *Proceedings of AMPT95*. pages 390–399.
- Boukouvalas, C., Kittler, J., Marik, R., and Petrou, M. (1999). Color grading of randomly textured ceramic tiles using color histograms. In *IEEE Transactions on Industry Electronics*. pages 219–226.
- Boukouvalas, C. and Petrou, M. (2000). Perceptual correction for color grading of random textures. In *Machine, Vision and Applications*. pages 129–136.
- Gottesfeld, L. (1992). A survey of image registration techniques. *ACM Computing Surveys*. pages 327–376.
- López, F., Acebrón, F., Valiente, J., and Perez, E. (2001). A study of registration methods for ceramic tile inspection purposes. In *Proc. of the IX Spanish Symposium on Pattern Recognition and Image Analysis*. pages 145–150.
- López, F., Valiente, J., Baldrich, R., and Vanrell, M. (2005). Fast surface grading using color statistics in the CIE Lab space. In *Iberian Conference on Pattern Recognition and Image Analysis*. In LNCS 3523. pages 666–673.
- Markou, M. and Singh, S. (2003). Novelty detection: a review - part 1: statistical approaches. In *Signal Processing* 83. pages 2481–2497.
- Smith, M., S. R. (2000). Automated inspection of textured ceramic tiles. In *Computers in Industry* 43. pages 73–82.
- Valiente, J., Acebrón, F., and López, F. (1998). An Automatic Visual Inspection System for Ceramic Tile Manufacturing Defects. In *Proc. IASTED Int. Conf. on Signal Processing and Communications*. pages 257–260.
- Xie, X. (2008). A Review of Recent Advances in Surface Defect Detection using Texture analysis Techniques. In *Electronic Letters on Computer Vision and Image Analysis*. pages 1–22.